The water vapour flux above Switzerland and its role in the August 2005 extreme precipitation and flooding

ERNEST N'DRI KOFFI[1,3,*], EDWARD GRAHAM[1,2] and CHRISTIAN MÄTZLER[1]

[1] Institute of Applied Physics, University of Bern, 3102 Bern, Switzerland
[2] Lews Castle College, University of the Highlands and Islands, Stornoway, Scotland, HS2 0XR
[3] Current affiliation: European Commission Joint Research Centre, Institute for Environment and Sustainability, 21027 Ispra, Italy

Abstract

The water budget approach is applied to an atmospheric box above Switzerland (hereafter referred to as the "Swiss box") to quantify the atmospheric water vapour flux using ECMWF ERA-Interim reanalyses. The results confirm that the water vapour flux through the Swiss box is highly temporally variable, ranging from 1 to 5×10^7 kg/s during settled anticyclonic weather, but increasing in size by a factor of ten or more during high speed currents of water vapour. Overall, Switzerland and the Swiss box "import" more water vapour than it "exports", but the amount gained remains only a small fraction (1% to 5%) of the total available water vapour passing by. High inward water vapour fluxes are not necessarily linked to high precipitation episodes. The water vapour flux during the August 2005 floods, which caused severe damage in central Switzerland, is examined and an assessment is made of the computed water vapour fluxes compared to high spatio-temporal rain gauge and radar observations. About 25% of the incoming water vapour flux was stored in Switzerland. The computed water vapour fluxes from ECMWF data compare well with the mean rain gauge observations and the combined rain-gauge radar precipitation products.

Keywords: Switzerland, Water vapour flux, Mass balance theory, Water budget, Radar, Rain gauges, ECMWF ERA-Interim, August 2005 floods.

1 Introduction

Quantification of precipitation has been one of the greatest challenges meteorologists have faced. Rain gauges provide only point measurements of precipitation-rate and weather radars do not provide direct measurements. Both methods have difficulties or fail in mountainous regions, such as, for example, in the Swiss Alps (GERMANN et al., 2006). At the same time, meteorological analyses based on observations are becoming more and more reliable (*e.g.* UPPALA et al., 2005; DEE et al., 2011). Analyses are based on the mass balance equation by using meteorological fields observed either on the ground, from balloons in the atmosphere, or determined by satellite sensors in space. Indeed, an analysis is an optimum fit between a short-term model prediction and observations, whilst taking into account the errors in the model and in the observations. The method to produce the analysis is termed an assimilation technique. Thus, using measurements of the wind, humidity, air temperature and radiation, these sparse observations can be extended onto a grid at both horizontal and vertical scales and through time for many years. In this study, we investigate the water budget approach to estimate precipitation during active meteorological situations over a box that encompasses Switzerland. It is well known that such events quickly transport water vapour over a given domain, and therefore the loss of water vapour in such conditions should be related to the precipitation measured on the ground within that domain. The primary objective of this work was a unique study of the water vapour budget above a box encompassing Switzerland to help understand the causes of the extreme floods which devastated the central part of the country in August 2005.

The basic concept of using the atmospheric data to estimate components of the mass balance was first formulated by BENTON and ESTOQUE (1954) and STARR and PEIXOTO (1958), followed later by several other studies (*e.g.* HASTERNRATH, 1986; SAHA and BAVADEKAR, 1973; CADET and REVERDIN, 1981, and references herein. All these earlier studies used limited gridded data from coarse observation networks. In recent years, thanks to the improved assimilation techniques used to generate gridded analyses at high spatial and temporal resolutions, interest in such studies have increased again among the scientific community. Thus, by using the National Centers for Environmental Prediction (NCEP) and the European Centre for Medium Range Weather Forecasts (ECMWF) reanalyses, many studies have focused on the hydrological cycle over specific regions such as in Africa (*e.g.* MATSUYAMA et al., 1994; SIMMONDS et al., 1999), the Amazon Basin (*e.g.* BRUBAKER et al.,

*Corresponding author: Ernest N'Dri Koffi, Institute of Applied Physics, University of Bern, Sidlerstrasse 5, 3012 Bern, Switzerland, e-mail: ernest.koffi@jrc.ec.europe.eu

1993), North America (*e.g.* SMIRNOV and MOORE, 1999; SENEVIRATNE et al., 2004; ZANGVIL et al., 2010), China (SIMMONDS et al., 1999; ZHOU and YU, 2005), Antarctica (*e.g.* CONNOLLEY and KING, 1993; CULLATHER et al., 1996), Europe (*e.g.* PHILLIPS and MCGREGOR, 2001), Eurasia (*e.g.* BRUBAKER et al., 1993), and the Pacific (*e.g.* KHATEP et al., 1984). The regional hydrological cycle, including precipitation, stream flow, and surface evaporation were commonly investigated. Moreover, regional water vapour fluxes have been related to observed rainfall. As an example of the studies mentioned above, KHATEP et al. (1984) analysed the water vapour flux over the southwest Pacific in the context of rainfall variations over New Zealand between 1960 and 1973. The results showed that drought and wet periods over this country were found to be related to the origin of water vapour transfer. SIMMONDS and HOPE (1998) compared the transport of water vapour into southeast and northeast China during summer monsoon. The mass balance approach worked fairly well when comparing observed rainfall to the calculated water flux convergence, but the authors highlighted an additional difficulty due to the extent that irrigation over China had on the moisture budget. TRENBERTH and GUILLEMOT (1996) explained the 1988 US drought and 1993 Mississippi floods in terms of an interplay between the water vapour flux, the latitude of the jet stream, and air pressure systems. MATSUYAMA et al. (1994) described seasonal changes in the water budget of the Congo River basin in Africa. PHILIPS and MCGREGOR (2001) assessed the sensitivity of a regional rainfall index for southwest England in relation to the water vapour flux over western Europe on a monthly timescale. The results revealed a strong association between westerly water vapour flux and southwest England rainfall. BRUBAKER et al. (1993), by using the convergence of atmospheric water vapour over four continental regions (North America, South America, Eurasia, West Africa) together with a simplified model of the atmospheric moisture, estimated the contribution of regional evaporation to regional precipitation. For the regions studied, the ratio of locally contributed to total monthly precipitation was found to generally lie between 0.1 and 0.3, but can reach up to 0.48 in Africa. Of course, for a meteorological event, this ratio can be dominated by an airmass purely advected into the domain (close to 0) or by only local air mass convection (tendency to 1).

Significant discrepancies have been obtained between different gridded operational analyses. These uncertainties are due to various reasons such as the different treatment of physical process, the model topography, gaps in the data used, and uncertainties in the moisture and wind analyses, with the wind field being the most significant of uncertainty (WANG and PAEGLE, 1996).

Previous studies have mainly used statistics of the long-term mean or seasonal cycles to characterise results. Thus, mean water vapour fluxes have been often correlated to observed rainfall, instead of comparing their absolute values or magnitudes to rainfall intensity. Here, we use six-hourly values of water vapour from the ECMWF analyses to compute the water vapour flux in space and time and thus the water vapour transport, to provide new insight into the fluctuations which characterise the meteorological events associated with precipitation. We consider a box that encompasses Switzerland (hereafter referred to as the "Swiss box") to estimate the water budget. We have focused on active frontal (windy) meteorological events that transport the water vapour quickly, allowing us to relate the water vapour flux convergence to the observed precipitation measured on the ground by neglecting the part of the precipitation caused by local land evapotranspiration. Such meteorological events were observed during the disastrous floods of late August 2005 which brought great damage to large parts of Switzerland. We use the water budget approach to estimate precipitation without local contribution. We then compare these estimates to the rain gauges and weather radar observations. It is worth noting that when we started this study, we intended to compute the water vapour fluxes by using Global Positioning System (GPS) integrated water vapour (W) data, which have been studied for many years using the data archive at the Institute of Applied Physics at the University of Bern, Switzerland (e.g. GUEROVA et al., 2005; MORLAND and MÄTZLER, 2007), but we quickly realised that the water vapour flux cannot be obtained reliably from the W data because the horizontal wind speed varies with altitude.

This paper is organized as follows: In the next section, we recall the mass balance theory and outline our methodology to compute the water vapour flux. In section 3, the calculated water vapour fluxes for the whole year of 2006 as illustrations of representative water vapour budget variations over the Swiss box are presented and discussed, followed by a closer look at the disastrous flood events of August 2005 in Switzerland in the form of case-study. Our overall conclusions are then presented in Section 4.

2 Theory, methodology and data

2.1 Theory: The mass balance of the Swiss atmospheric water

The "mass balance" of the atmospheric water system can be described, at any moment in time, by means of the equation:

$$\frac{\partial W}{\partial t} = AW_{in} - AW_{out} + E - P \qquad (1)$$

where t is the time, and W is the combined integrated water vapour, integrated cloud liquid water, and the integrated cloud solid (ice) water both in vertical direction and over the entire volume of the "Swiss box" (E and P stand for evaporation and precipitation, respectively). AW is the atmospheric water flux (liquid and solid water and water vapour) passing into (denoted by subscript *in*), or out of (denoted by subscript *out*), pre-defined boundaries of the Swiss Box. As an example, the integrated water vapour is defined by:

$$W = \int_y \int_x \left(\int_{P_{top}}^{p_s} \frac{qdp}{g} \right) dxdy \qquad (2)$$

where q is the specific humidity, p is the pressure, g is the acceleration of gravity, p_s is the surface pressure, and p_{top} is the pressure at the top of the atmosphere. x and y represent the eastward, northward directions of the borders of the box. Equation (2) can also be used for both the integrated liquid water and ice water by replacing the specific humidity with the specific cloud liquid water or the specific cloud ice water, respectively.

Some of the water within the Swiss box can be, *(i)* put into storage (*i.e.* lost by precipitation), or *(ii)* taken from storage (*i.e.* gain by evaporation). One must consider water vapour in gas form, as well as liquid or solid water (ice) in the form of suspended precipitation or cloud droplets or crystals moving across the borders into, or out of, the Swiss box at a particular time in question. Taking these factors into account, the mass balance equation (Equation (1)) therefore now becomes, for the whole depth of the atmosphere:

$$P - E = \left[-\frac{\partial W}{\partial t} + (Wv_{in} - Wv_{out}) \right]$$
$$\text{(I)} \qquad\qquad \text{(II)}$$
$$+ \left[-\frac{\partial W_L}{\partial t} + (Lw_{in} - Lw_{out}) \right]$$
$$\text{(III)}$$
$$+ \left[-\frac{\partial W_I}{\partial t} + (Iw_{in} - Iw_{out}) \right] \qquad (3)$$
$$\text{(IV)}$$

where Wv is the atmospheric water vapour flux, E is gain by evaporation, P is loss through precipitation, Lw the liquid water flux (cloud droplets and precipitation), and Iw the solid water flux (ice crystals). The subscripts *in* and *out* refer to the respective flux into *(in)* or out of *(out)* Switzerland. W_L and W_I are the integrated liquid water and solid and water, respectively. The terms (II), (III), and (IV) stand for the contributions of water vapour, liquid water, and solid (ice) water to the total atmospheric water fluxes over the studied basin, respectively.

Details on the formulation of the Equation (3) and some approximations can be found in BENTON and ESTOQUE (1954), STARR and PEIXOTO (1958), SCHMITZ and MULLEN (1996), and SMIRNOV and MOORE (1999). Equation (3) can also be described by means of a three-dimensional diagram (Fig. 1), which considers Switzerland (and the atmosphere above it) as a six-sided
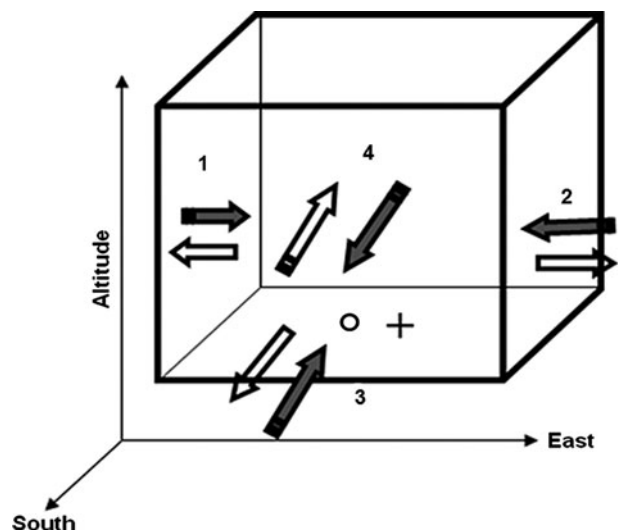

Figure 1: A schematic diagram, depicting the box encompassing Switzerland (and the atmosphere above the country) as a three-dimensional box (called "Swiss box"), with fluxes of atmospheric water (combined ice, liquid and vapour) into and out of each side of the box indicated by the filled-in (into) and hollow (out of) arrows. The black circle and cross on the floor of the box indicate the evaporation and precipitation fluxes, respectively, between the ground and the atmosphere. It is assumed that there are no fluxes either out of, or into, the top (ceiling) of the box *i.e.* no escape to, or entry from the stratosphere. The sides of the "Swiss box" are numbered.

box (*aka* the "Swiss box"), with a flux of atmospheric water in and out of each vertically orientated side of the box (as indicated by the arrows, respectively).

We initially computed the contributions of liquid water and solid water and our results show that they amount to only a few percent or less of Wv_{in} or Wv_{out}, and therefore can be ignored for the basis of a study like this. Indeed, overall the computed liquid water and ice water fluxes are found to be at least 10 times smaller than water vapor fluxes (See supplementary material). To avoid examining a large amount of data for a little extra benefit, we therefore considered a simplified mass balance equation that reads as follows:

$$P - E \approx -\frac{\partial W}{\partial t} + (Wv_{in} - Wv_{out}) \qquad (4)$$

The right hand side of Equation (4) is used in this study to confront to observed precipitation in Switzerland when evaporation is minimal (i.e., $E \approx 0$). The two components on the right hand side of Equation (4) (i.e., the temporal variation of the integrated water vapor and the water vapor fluxes) are computed by using the following method and data.

2.2 Methodology and data

The atmospheric water vapour flux Wv in y direction over the Swiss box is expressed as follows:

$$Wv_y = \int_x \left(\int_{P_{top}}^{p_s} \frac{qU_y dp}{g} \right) dx \qquad (5)$$

where U_y is the component of the horizontal wind vector in y direction. An equivalent equation holds for the x direction.

As shown in Fig. 1, we assume that there are no fluxes into, or out of, the horizontal top boundary of the box (equivalent to escape or arrival from the stratosphere). This assumption is reasonable since at the top of our "Swiss box" (set at 150 hPa), the specific humidity is very low and therefore the vertical exchanges of water vapour fluxes through this level are negligible. There are, however, important fluxes between the bottom floor of the box and the atmosphere above it, namely precipitation and evaporation (these are indicated by the circle and plus signs on the floor of the box).

Specific humidity, horizontal wind vectors, air temperature, and geopotential data from the ECMWF ERA-interim reanalysis (DEE et al., 2011) at a horizontal resolution of 0.5 degree (latitude/longitude) were retrieved at six-hourly resolution for the complete years of 2005 and 2006, for the area encompassing latitudes 46.0 to 48.0° N and longitudes 6.0 to 10.5° E. Data was retrieved from 15 vertical pressure levels of the ECMWF model, with the top level at 150 hPa. The bottom level was set to the model's orography (shown in Fig. 3). The corners of the Swiss box were defined, as depicted in Fig. 2.

Using the ECMWF data, the fluxes of Wv_{in} and Wv_{out} for each vertical side of the "Swiss box" in Equation (4) were calculated for successive six-hourly periods by calculating the product of the water vapour density (kg/m³; derived from the specific humidity [kg/kg] and airmass density [kg/m³]) multiplied by the windspeed (m/s) for each grid square, and integrating over the horizontal

and vertical dimensions of the box side. Thus, referring again to Fig. 1, the Wv_{in} and Wv_{out} fluxes correspond to the following numbered "sides" of the Swiss box:

$$Wv_{in} = 1 - 2 + 3 - 4$$
$$Wv_{out} = -1 + 2 - 3 + 4$$

We computed Wv_{in} and Wv_{out} by using rectangular coordinates x, y, z. Thus, we converted the pressure levels of ECMWF analyses to altitudes z. We consider a hydrostatic assumption, which allows the variation of the pressure dp as a function of the variation of the altitude dz. Wv_{in} and Wv_{out} are then derived from the Equation (5) as follows:

$$\begin{cases} \text{Flux at 1 and 2}: \int_z \int_y \rho_w U_x dy dz \\ \text{Flux at 3 and 4}: \int_z \int_x \rho_w U_y dx dz \end{cases} \qquad (6)$$

where U_x and U_y are the West-East (positive) and South-North (positive) wind components respectively, and ρ_w is the water vapour density and x, y and z represent the eastward, northward and vertical directions by considering the Earth as a sphere. The altitude z is derived from the geopotential of ECMWF data divided by the acceleration of the gravity g. Thus for example, the water vapour flux through side 1 of the Swiss box (*i.e.* west side) is the integral (in y and z directions) of the product of the wind speed and water vapour density of each grid square. Due to the conversion of pressure levels to z altitudes, when computing Wv_{in} and Wv_{out}, only surface data having altitude greater than the model's orographic height were used. This can underestimate locally the computed water vapour flux near the ground for meteorological events with actual high surface wind speeds, but the averaging over the Swiss box may limit this effect.

Given the six-hourly time resolution, the ability of the ECMWF model to capture transient water vapour features can be estimated, by considering a moderate mid-tropospheric wind of say, 20m/sec (72 km/hr). In this way, a transient water vapour feature traversing Switzerland (about 350 km wide from west to east) in an orthogonal direction would spend only 5 hours in the skies above the country, before moving out of the country again (this crossing time is smaller for wind blowing from north to south, where the horizontal extension is about 200 km). Even if the full mesoscale features of atmospheric water ("peaks") can hardly be captured by the ECMWF model data at a 6 hour time interval, we have computed the integrated water vapour tendency ($\partial W / \partial t$; see Equation (3)) from the slope between two consecutive values of the mean integrated water vapour computed over the Swiss box. As already stated, the primary objective of this work was a unique study of Switzerland itself to help understand the water vapour budget during the extreme floods episode of August 2005 which devastated central Switzerland. However, the same procedures and methods could easily be used for a larger area in the future.

Figure 2: A map of Switzerland showing the locations of the 70 rain gauge stations of the MeteoSwiss surface meteorological network (ANETZ, are indicated by open circles). The three C-band Doppler precipitation radars of MeteoSwiss used in this study are located on mountain tops, near Zurich on Albis (925 m above sea level (ASL)), near Geneva on La Dôle (1675 m ASL), and near Lugano on Monte Lema (1625 m ASL) are depicted by filled squares.
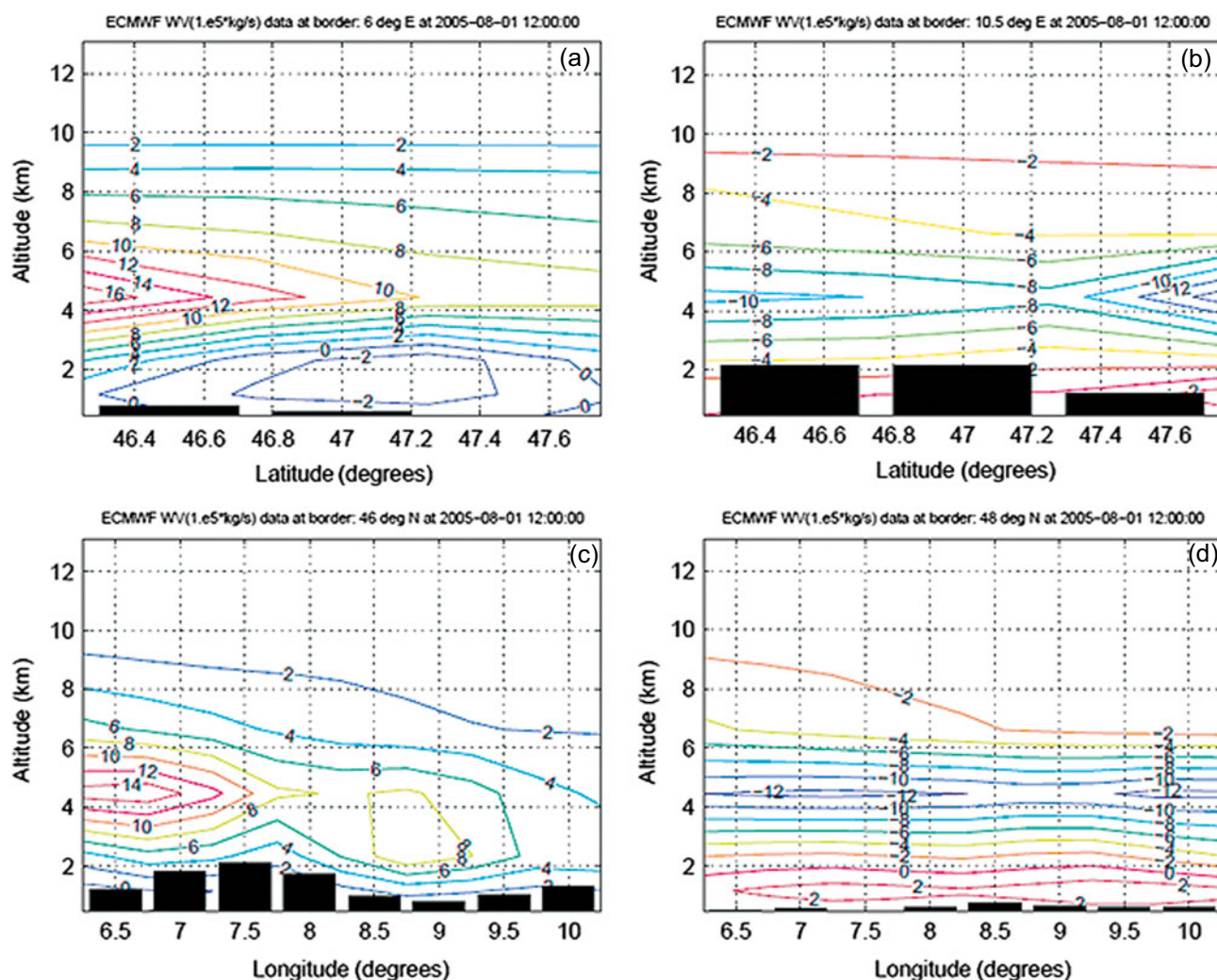
Figure 3: Cross section of ECMWF model water vapour flux (10^5 kg/sec) at 12 UTC on 1 August 2005 passing through each vertical side of the Swiss box (CH), with height (km) plotted on the Y-axis; a): west border at 6° E; b): east border at 10.5° E; c): south border at 46° N; d): north border at 48° N. The computed fluxes are representative of the area of their relevant grid box (which is 0.5° lat or 0.5° lon multiplied by the distance between two ECMWF vertical levels). The black column bars in each plot represent the ECMWF model topography. Negative values of water vapour flux mean that water vapour is leaving the Swiss box region.

The remaining parts of the Equation (4), namely E (evaporation), P (precipitation) can now be estimated or measured by other means, by using *e.g.* Swiss National Meteorological Service (MeteoSwiss) radar and the MeteoSwiss Automatisches MessNetz (ANETZ) observational precipitation network data (Fig. 2). In the case of very heavy rainfall and low air temperature (such as during the August 2005 flood event), E (evaporation) can be considered to be minimal or close to zero. In fact, we estimated the evaporative flux in Switzerland under these conditions to be at most 1×10^6 kg/s, which accounts for no more than a few percentage of the total water vapour flux. This was obtained from the ECMWF ERA-Interim analyses relevant for the instantaneous moisture flux at the surface.

Considering the above assumptions, Equation (4) was tested and calculated using ECMWF analyses,

MeteoSwiss ANETZ rain gauges and two MeteoSwiss combined radar rain-gauge rainfall products. These products are: i) The combined radar and rain-gauge data that were specifically generated for the flood event in August 2005 (FREI et al., 2006; FREI et al., 2008). These data are hourly-aggregated raingauge-adjusted radar maps (resolution 1 km^2). This radar product is called RADAR hereafter. ii) The recently developped product that combines in real-time radar and rain-gauge measurements using a co-kriging-with-external-drift technique for hourly rainfall accumulations (SIDERIS et al., accepted). The algorithm relevant for this new product has been applied to generate the data for the August 2005 flood event. These data are called hereafter CPC data. The technical specifications and the methodology of data processing of the MeteoSwiss radar data can be found in *e.g.* JOSS et al. (1997) and GERMANN et al. (2006). It is worth noting

that these data are derived from composite images recorded from 3 radars, as shown in Fig. 2. The algorithm used for estimating precipitation rate from the MeteoSwiss radar data includes some direct ground-truthing by precipitation gauge measurements, but also includes the use of some cloud physics to infer the precipitation rate in sheltered Alpine valleys where the radar beam cannot penetrate (GERMANN et al., 2006). Of particular interest was whether Equation (4) could be made to balance, and whether the estimated precipitation part on the right side of Equation (4) (*i.e.* water lost) equalled that measured in the ANETZ rain gauges, or the estimations by the MeteoSwiss combined rain-gauge and radar rainfall products.

3   Results and discussions

This section presents a selection of results of applying the theory and methodology outlined in sections 1 and 2 to determine the water vapour flux through Switzerland for the month of August 2005 and also the complete year of 2006. The year 2006 was selected because it is representative of the mean water vapour characteristics over the Swiss box (See supplementary material) and it is also the year just after 2005 when Switzerland was hit by the severe August flood event. The results are then discussed in detail with regard to the prevailing meteorological conditions of the time in question. After this, section 3.3 takes a closer look at the Swiss flood episode of 18-23 August 2005.

3.1   Introductory results and features

As an illustration of representative water vapour budget over Switzerland, Fig. 3 shows the ECMWF analyses water vapour flux (kg/s) at 12 UTC on 1 August 2005, with height (kilometres) plotted on the Y-axis; ([a]: west border at 6°E; [b]: east border at 10.5°E; [c]: south border at 46°N; [d]: north border at 48°N). The computed fluxes are representative of the area of the side of relevant grid-box through which the flux occurs (*i.e.* 0.5°lat or 0.5°lon times the difference between two ECMWF vertical levels *[m]*). The black columns in each plot represent the ECMWF model topography, which is a very coarse approximation. Negative values of water vapour flux mean that water vapour is leaving the Swiss box, while positive values show that water vapour is entering. Note the reasonably high water vapour fluxes of up to 1.6×10^6 kg/s between 4 and 6 km in height (in image *[a]*), despite there being considerably less water vapour normally at these heights compared to the near-surface. This is because there is a strong north-west wind at these altitudes, continuously advecting in water vapour at a rapid rate.

Fig. 4 shows the same diagram as Fig. 3, but for the following day 2 August 2005 at 12UTC. Note the strong positive water vapour values of over 3×10^6 kg/s around

2-6 km in height, centred at 10.0° E in image [c] (southern Swiss border at 46.0°N), and the corresponding strong negative values of -2.5×10^6 kg/s at the same height/longitude in image [d] (northern Swiss border at 48°N). These may indicate the occurrence of a narrow mid-tropospheric water vapour "jet" or a "*warm conveyer belt*" (NEIMAN et al., 2008). These usually occur on the eastward side of a Rossby wave trough, and ahead of the advancing cold front of a mid-latitude weather system.

3.2   The Swiss water vapour flux for the year 2006

Plots of the water vapour flux over Switzerland for each six-hourly period for the whole year of 2006 are presented in Fig. 5. The water vapour flux into Switzerland (Wv_{in}) is plotted as a black line, whilst the water vapour flux out of Switzerland (Wv_{out}) is plotted as a dark blue-dashed line. The difference between the two (*i.e.* Wv_{in}-Wv_{out}) is shown in dashed-red line. The following features can be noticed almost immediately from this Figure.

Wv_{in} and Wv_{out} are extremely variable, typically ranging from 0.2 to 0.5×10^8 kg/s during settled anticyclonic spells of weather, but rising abruptly to 1.0 or 1.5×10^8 kg/s during short spells of weather every few weeks, and as high as 2.5×10^8 kg/s (*i.e.* 0.25×10^6 m^3/s) such as in early October 2006. Note that the most extreme peaks occur during the warmer part of the year from June to November. This extreme variation in values is to be expected, as the water vapour flux through Switzerland is most strongly controlled by windspeed in the middle and upper troposphere. High-speed currents of water vapour, already referred to as "*warm air conveyer belts*" or "*atmospheric rivers*" (*e.g.* NEIMAN et al., 2008) are well known features of the warm-frontal zones of Atlantic depressions, and pass by Switzerland fairly regularly. Following this "river" analogy a little further, the computed maximum of water vapour flux Wv_{in} is 0.25 *Sv*, which is about 20% of the net outflow of all the rivers in the world (DAI and TRENBERTH., 2002). Note that *Sv*, which is the unit of Sverdrup equals 10^6 m^3/s. Each peak in the Wv_{in} curve represents one of these transient features passing by Switzerland. Wv_{in} is generally greater than Wv_{out} at most times, also shown by the fact that the difference between the two (red line in Figs. 5) lies generally above zero. However, the difference is only a small fraction (1% to 5%) of the total Wv_{in}. This fraction increases a little when considering the contributions of both liquid water and solid water. Indeed, on average and at annual scale, the Swiss box also imports liquid water and solid water, which is estimated to be about 1% of the incoming water vapour flux (See supplementary material).

As for ($Wv_{in} - Wv_{out}$), the integrated water vapour tendency $(-\partial W/\partial t)$ is also found to be highly variable, as shown in Figs. 6(a) and 7. Values of $(-\partial W/\partial t)$ are
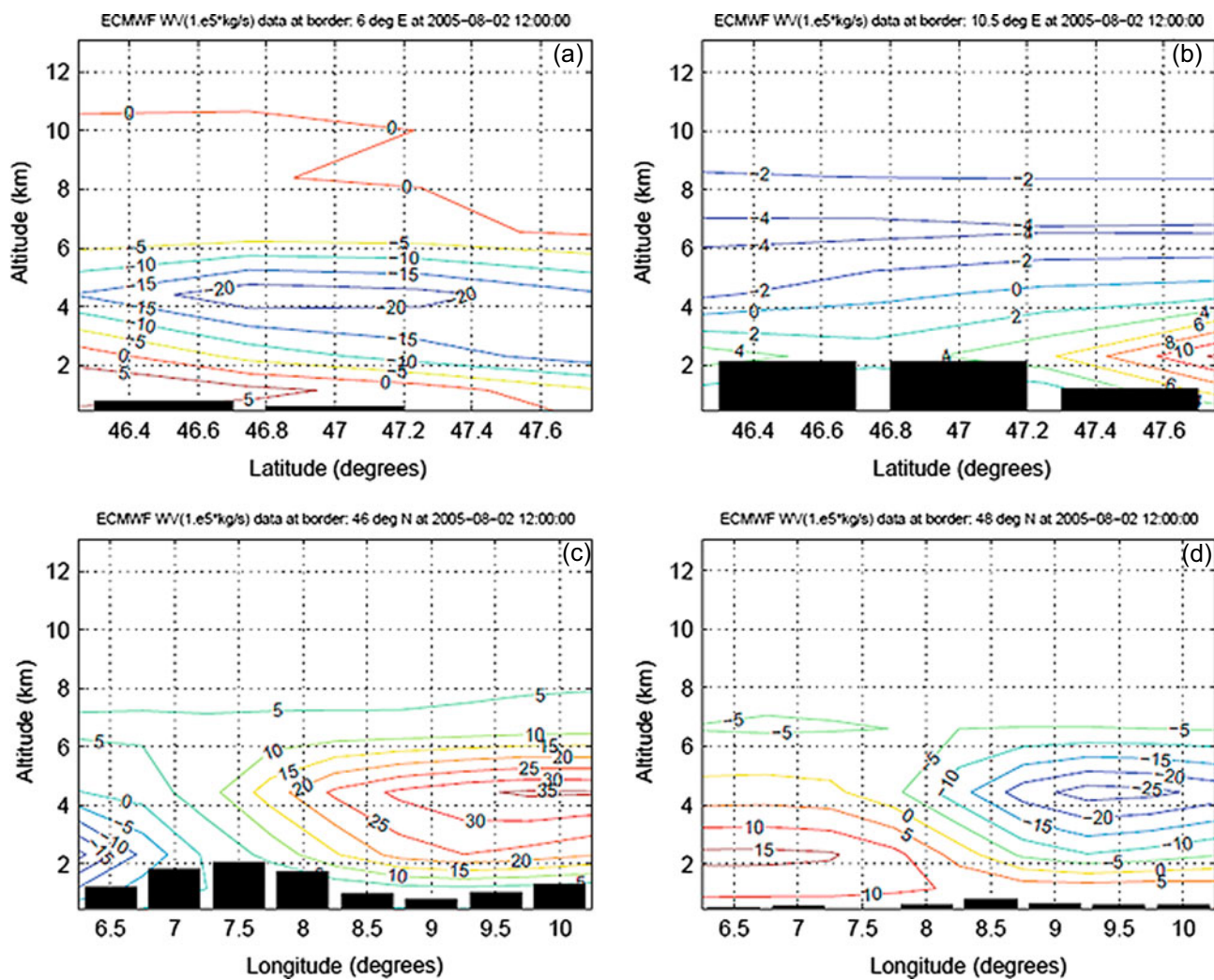
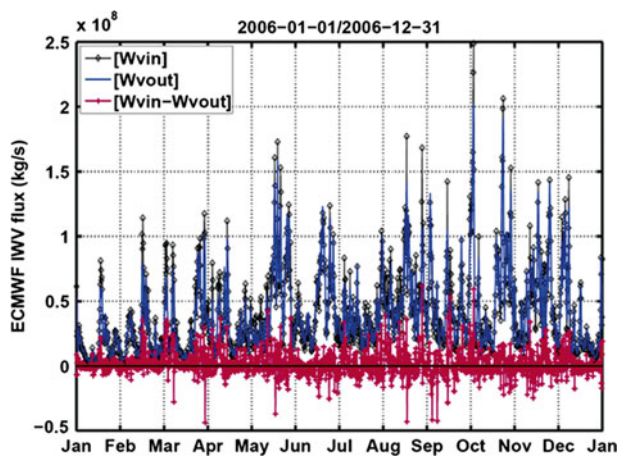**Figure 4:** Same as Figure 3 but for 12 UTC on 2 August 2005.

Figure 5: ECMWF model flux of water vapour (kg/sec) into the Swiss box (Wv_{in}, black solid line with open diamonds), flux of water vapour out of Switzerland (Wv_{out}, blue solid line), and their difference $Wv_{in}-Wv_{out}$ (red solid line with crosses) for each six-hourly period of the whole year of 2006.

in the same order of magnitude of $Wv_{in} - Wv_{out}$, especially for relatively small $Wv_{in} - Wv_{out}$ values. The term $(-\partial W/\partial t)$ and $Wv_{in} - Wv_{out}$ are fairly well anti-correlated, especially when the two quantities show large values. As can be seen from the Figs. 6a and 7, minima of $(-\partial W/\partial t)$ often coincide with maxima of $(Wv_{in} - Wv_{out})$ and vice versa. These results are in agreement with those reported by SMIRNOV and MOORE (1999) who studied water vapour transport in the Mackenzie River Basin and used ECMWF analyses with the same time intervals, and with a relatively coarse spatial resolution (1.125° spacing). A strong anti-correlation between $(-\partial W/\partial t)$ and $(Wv_{in} - Wv_{out})$ can occur when most of the incoming water vapour that entered in the studied basin remains and does not precipitate (i.e., $P = 0$). Thus, the integrated water vapour increases, giving an increase of its tendency. Consequently, $(-\partial W/\partial t)$ is in opposite phase with $(Wv_{in} - Wv_{out})$.

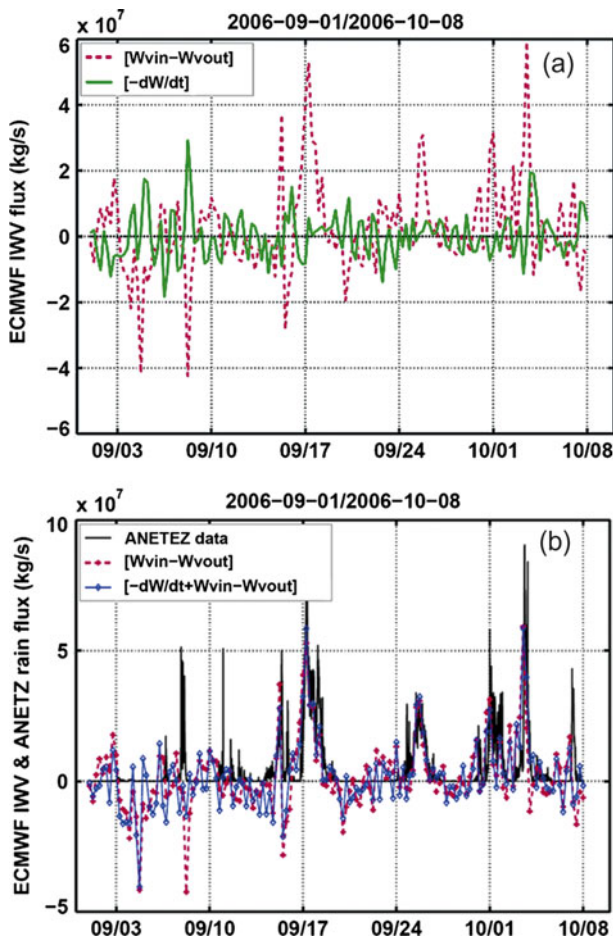On average, for the whole year of 2006, some atmospheric water vapour was stored in Switzerland and this

Figure 6: a) ECMWF modelled water vapour tendency (kg/sec) into the Swiss box (Wv_{in}-Wv_{out}; red dashed line), and the integrated water vapour tendency ($-\partial W/\partial t$, green solid line) for each six-hourly period of September and early October 2006 (month/day on the horizontal axis) are shown. b) $Wv_{in} - Wv_{out}$ (red dashed line with crosses) and ($-\partial W/\partial t + Wv_{in} - Wv_{out}$) (blue solid line with open diamonds) for the same period, but compared to the MeteoSwiss ANETZ 10-minute (black solid line) ground precipitation observations calculated as the mean ANETZ rainfall rate of all available stations multiplied by same area of the Swiss box used to compute the water vapour fluxes.

Figure 7: Case study of the August 2005 floods: The total ECMWF water vapour (W) flux tendency (kg/sec) for the Swiss box for the complete month of August 2005 (day of month on horizontal axis), for ($Wv_{in} - Wv_{out}$, red dashed line with crosses) and the integrated water vapour tendency tendency ($-\partial W/\partial t$, green solid line).

feed surrounding countries, mainly along the Rhine, the Rhone, the Ticino, and the Inn Rivers, respectively.

These findings should not be taken with great surprise, because Switzerland is a mountainous country, and mountains can be very efficient at extracting water vapour, particularly in strong wind situations typical of atmospheric rivers (by substantial orographic enhancement of precipitation).

Another important finding is that high Wv_{in} values are not necessarily linked to high precipitation episodes. For example the very high values of 2.5×10^8 kg/s in early October 2006 (Fig. 5 and Fig. 6a) were coincident with very mild, moist south-westerly winds, but total precipitation was not extreme. A mechanism to enhance precipitation is also needed. In fact, one can speculate that *e.g.* precipitation downdraughts as well as and the complex orography in the Swiss box can enhance convection to cause precipitation by lifting low-level humid airmass aloft.

As expected, large positive values of ($-\partial W/\partial t + Wv_{in} - Wv_{out}$) correlate well with the observed ANETZ rain gauge data (Fig. 6(b)). However, small positive values of this quantity without precipitation might be explained by the uncertainties in the ERA-Interim wind field as well as the contributions due to evaporation, liquid water fluxes, and solid water fluxes, which we have neglected. WANG and PAEGLE (1996) reported important uncertainties in wind fields when using ERA-40, but DEE et al. (2011) evaluated the ERA-Interim analyses with respect to ERA-40 and found significant improvements (including in the wind fields). Furthermore, the other quantities neglected in the Equation (3) (*i.e.* evaporation, liquid and ice water flux, vertical transport of the water vapour out of the top of the Swiss box) as well the method used to compute the integrated water

storage was dominated by the water vapour flux ($Wv_{in} - Wv_{out}$). The mean value of ($-\partial W/\partial t + Wv_{in} - Wv_{out}$) is found to be 1.6×10^6 kg/s, while a negative and residual value of the integrated water vapour tendency is obtained (-0.1×10^4 kg/s). Thus, as already reported in previous studies, for a long time interval, the term of integrated water vapour tendency ($-\partial W/\partial t$) in the mass balance equation (Equation (4)) can be neglected.

The mean positive value of ($Wv_{in} - Wv_{out}$) obtained means two things; *(a)* Switzerland "imports" more water than it "exports", but *(b)* the amount gained (*i.e.* through precipitation) remains only a small fraction of the total available water vapour passing by. Of course, in the exported water, however, we have neglected the contribution of rivers and ground water exiting Switzerland which
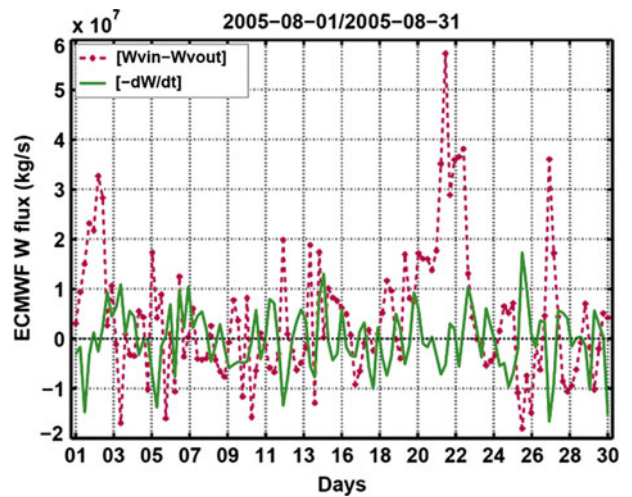
vapour tendency and water vapour flux may have contributed to these uncertainties. For example, computing the integrated water vapour tendency $(-\partial W/\partial t)$ at the ECMWF data time interval (*i.e.* every 6 hours) may give rise to uncertainties due to the large time step, as stated earlier. Hence, the values of $(-\partial W/\partial t)$ can be either underestimated or overestimated. Finally, one could use the ECMWF data for the forecast of precipitation from the mass balance theory, as the global precision on the computed quantity $(-\partial W/\partial t + Wv_{in} - Wv_{out})$ can be estimated by considering the cases for which $(-\partial W/\partial t + Wv_{in} - Wv_{out})$ values are positive without any observed precipitation. Large negative values of $(-\partial W/\partial t + Wv_{in} - Wv_{out})$ are found to be most common (but not always) during summer and earlier in autumn when evaporation is greatest (Switzerland is "exporting" most water vapour then). This statement seems to be supported by SIMMONDS and HOPE (1998) when investigating the seasonal and regional responses to changes in Australian soil moisture conditions. Such cases can be illustrated for the period around 4 September 2006 where large negative values $(-\partial W/\partial t + Wv_{in} - Wv_{out})$ are computed. By using the ERA-interim surface instantaneous moisture flux, we estimate an evaporation to be about 4.5×10^{6} kg/s during this period. This evaporation amounts to only 20% of the mean value of $(-\partial W/\partial t + Wv_{in} - Wv_{out})$ computed over this period. This result is not consistent with our water budget model since no precipitation was recorded during this period in the Swiss box in the database we are using. Note that the contributions of both liquid water and solid water fluxes are found to be small for this period. Consequently, this imbalance of the mass balance equation might be explained by an underestimate of the evaporation from ERA-Interim data. Precipitation mechanisms are largely controlled by convection at this time of year, of which evaporation plays a key role. Such a case is well depicted in Fig. 6(b) where an episode of negative values of $(-\partial W/\partial t + Wv_{in} - Wv_{out})$ coincided with a relatively large amount of precipitation during the period from 6-9th September 2006.

Further analysis using ERA-Interim data for the period 2004-2009 inclusive (provided in supplementary information) shows that the mean incoming water vapour flux is 6.7×10^{10} kg/s and only 1.8% of this quantity was stored in the Swiss box, or about 1.2×10^{9} kg/s. In addition to water vapour, results show also that the Swiss box stored both the liquid water and solid water. On average, the liquid water convergence in the Swiss box is found to be about 13% of the water vapour convergence, while this value is 7% for the solid water convergence.

3.3 Special case study of August 2005 floods

We performed a detailed study on water vapour fluxes inferred from our water budget model (Equation (4))
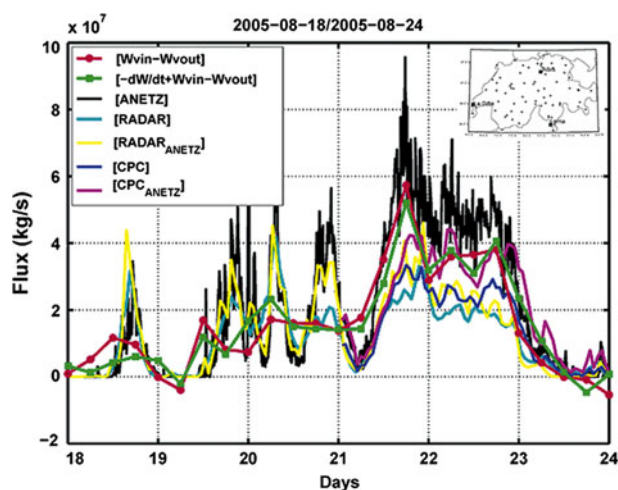

Figure 8: Case Study of the August 2005 floods: Modelled water fluxes ($Wv_{in} - Wv_{out}$; red solid line with filled circles) and ($-\partial W/\partial t + Wv_{in} - Wv_{out}$; green solid line with filled squares) for period of 18–24 August 2005 during a severe flood event in central Switzerland. The rain flux derived from MeteoSwiss ANETZ 10-minute ground observations (black solid line; ANETZ) is also shown; the ANETZ rain flux was calculated by multiplying the mean precipitation from all the 70 ANETZ sites by the area of he Swiss box (shown in the top right corner of the figure or see Figure 2). MeteoSwiss combined rain-gauge radar total instantaneous rainfall (kg/sec) for each hourly interval are also shown (denoted as RADAR; blue and cyan solid lines). RADAR were obtained using two different methods, namely (i) by calculating the sum of all the radar pixels over the Swiss box (cyan solid line), and (ii) using the radar precipitation pixel value closest to each of the 70 ANETZ sites (blue solid line; RADAR_ANETZ). As for RADAR data, the new product of MeteoSwiss radar-rain gauge data (denoted CPC) are also shown.

and for August 2005. We focused on the days of 18−23 August 2005 when a major flood episode affected Switzerland. To aid this part of the study, precipitation radar data was fortunately obtained from MeteoSwiss, together with MeteoSwiss ANETZ raingauge data from the University of Bern Institute of Applied Physics database.

Fig. 7 presents a similar graphic to Fig. 6(a), but for the month of August 2005 alone. The difference between the ECMWF inward and outgoing fluxes ($Wv_{in} - Wv_{out}$), and the integrated water vapour tendency $(-\partial W/\partial t)$ for the Swiss box for the complete month are shown. When ($-\partial W/\partial t + Wv_{in} - Wv_{out}$) exceeds zero, Switzerland may be gaining water through precipitation, and when it is less than zero, it means evaporation of water may be dominant. The main major flood peak can be seen from 21−23 August 2005; there is a large rise in ($Wv_{in} - Wv_{out}$) meaning there is less water vapour exiting Switzerland compared to that incoming. The shortfall in water vapour is of the order of 25−30%, meaning more than a quarter of the incoming water vapour may have been precipitated during the flood event.

Fig. 8 presents a zoom into the same results for the period of 18 to 24 August 2005. The computed water
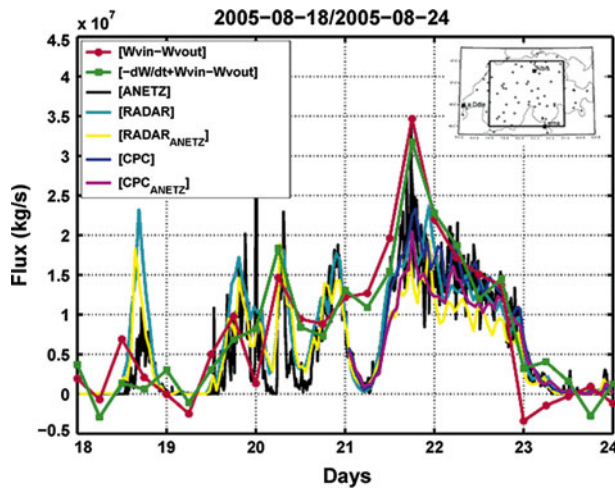
Figure 9: As Figure 8, but a medium spatial window shown on the top right corner of the graph is considered. The longitude/latitude coordinates of the left bottom and top right corners of the this spatial window are (7.0/46.0) and (9.5/47.5), respectively
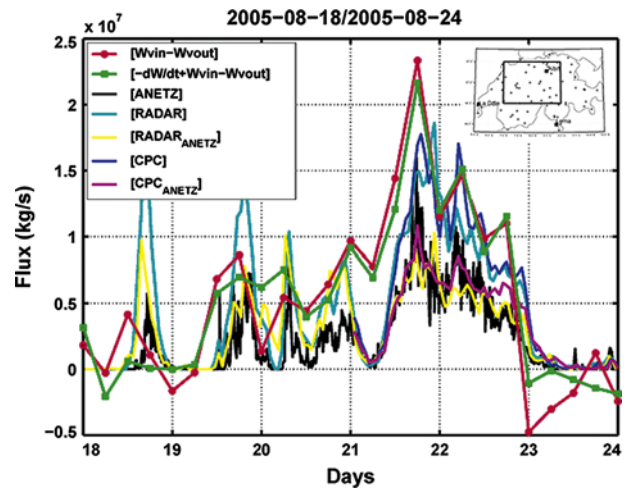

Figure 10: As Figure 8, but a small spatial window shown on the top right corner of the graph is considered. The longitude/latitude coordinates of the left bottom and top right corners of this window are (7.0/46.0) and (9.5/47.5), respectively.

flux convergence is compared to observed data derived from MeteoSwiss ANETZ 10-minute ground rain gauges. The observed data are calculated as the mean ANETZ rainfall rate of all 70 stations multiplied by the same area of the Swiss box used to compute the Wv_{in} and Wv_{out} fluxes. These show a good agreement overall with $(-\partial W/\partial t + Wv_{in} - Wv_{out})$. Indeed, the ANETZ curve almost mirrors the $(-\partial W/\partial t + Wv_{in} - Wv_{out})$ at all times, especially during the flooding rains of $21-23$ August. Moreover, as can be seen from Fig. 7, the integrated water vapour tendency $(-\partial W/\partial t)$ is small for this meteorological event and therefore can be neglected.

The peaks in the ANETZ data on the 18th August are thought to be due to convective storms forming and decaying within the Swiss boundaries, and thus do not appear on the $(-\partial W/\partial t + Wv_{in} - Wv_{out})$ trace (*i.e.* a whole evaporation-condensation-precipitation hydrological cycle is contained with the Swiss box). Meanwhile, the high frequency fluctuations late on the 20th and early on the 21st August are thought to be due to water entering Switzerland from the south as precipitation (GRAHAM et al. 2010).

Furthermore, the modelled water vapour flux $(-\partial W/\partial t + Wv_{in} - Wv_{out})$ is compared to the two MeteoSwiss combined rain-gauges and radar (i.e., RADAR and CPC; see section 2.2 for details) total rainfall (kg/s) over the Swiss box in two ways, as follows: Firstly, we considered the total rainfall from all the radar pixels in the Swiss box, and secondly, Only the radar pixel closest to the 70 sites of the ANETZ rain gauges were used to compute the mean precipitation before being then multiplied by the whole area for the Swiss box. The radar rainfall totals over the Swiss box for each hourly interval are in fairly good agreement with the modelled $(-\partial W/\partial t + Wv_{in} - Wv_{out})$ (Fig. 8), with better correspondence when considering the second method, (ii).

When focussing on the $21-23$ August 2005 episode during the severe weather event, the radar rainfall fluxes are lower than the modelled water flux derived from ECMWF analyses (*i.e.* $-\partial W/\partial t + Wv_{in} - Wv_{out}$). The differences between radar data and modelled water flux may be explained as follows: (i) The conversion of excess water vapour into precipitation ("precipitation efficiency") may not be constant in space and time; (ii) evaporation was greater than initially thought during the event, and (iii) other numerous inaccuracies, such as those already mentioned, due to the broad assumptions we made in our budget model (Equation (4)); both the contributions of liquid and solid water quantities are neglected) as well as the uncertainties in the quantities used to compute the water vapor fluxes (wind, humidity). But the fact that our $(-\partial W/\partial t + Wv_{in} - Wv_{out})$ data correspond closely to the MeteoSwiss radar precipitation values is very reassuring, however.

Particular attention was paid to the active meteorological events of $21-23$ August 2005 that transported the water vapour quickly over Switzerland. Such events allow us to relate water vapour flux to the observed precipitation measured on the ground. The mean value of the computed 6-hourly water vapour fluxes $(-\partial W/\partial t + Wv_{in} - Wv_{out})$ from ECMWF data is found to be 0.32×10^8 kg/s. We have estimated the uncertainty in the modelled precipitation by computing the contributions of evaporation, liquid water, and solid water using ECMWF data. Results clearly show that these contributions are very small, with the modelled precipitation increasing by about 5%. The total modelled precipitation is in good agreement with rainfall observed from ANETZ rain gauge stations. Note that the parameterized rainfall by ECMWF model over the domain of study (i.e. 0.21×10^8 kg/s) is about 1.5 times lower than our estimate. Such an underestimation of the observed rainfall by

ECMWF model has also been reported in other mountainous areas in Wales and Scotland (DEE et al., 2011). However, the mean water vapour flux is found to be only 28% less than the mean rainfall observed from ANETZ rain gauges, while it is 32−44% in excess to the mean rainfall obtained from radar measurements according to the methods used to compute the rainfall over the Swiss box (see Fig. 8). Results show a relatively slight good agreement between CPC data and the modelled water fluxes. Derived mean rain rates over the Swiss box, by using water vapour fluxes and rain gauge measurements, are found to be about 1.5 and 1.9 mm/h, respectively, values that are comparable to those observed in tropical cyclones at this spatial scale (*e.g.* LONFAT et al., 2004).

The calculated water vapour fluxes were then correlated to the observed precipitation. Since the ANETZ rainfall are observed every 10-minutes and the precipitation radar data was available for every hour, we averaged the observations over 6 hours by using two time windows: rainfall that was observed within (i) the interval *[t − 3 h; t + 3 h]*, and (ii) that included in the interval *[t; t + 6 h]*, and are associated to water vapour flux computed at the time *t*. The time window (ii) might permit the avoidance of any bias between computed water vapour fluxes and observed rainfall. Indeed, as portrayed in Fig. 8, the exact timing of peaks in radar rainfall (here mainly from RADAR product) and water vapour fluxes do not coincide precisely during the period of 21–23 August. Precipitation data are not used in the ECMWF data assimilation process, therefore we assume that observed rainfall and the computed water vapour flux have reasonable independence. Hence, we have calculated the coefficients of linear regression between the computed and observed quantities. Whatever the time window selected to calculate the mean observed rainfall from ANETZ data, a relatively good and statistically significant (at least at $p = 0.05$) correlation was found between the water vapour flux and precipitation obtained from rain gauges: The coefficient of linear regression R is 0.92 for a paired size of 8 data points but becomes somewhat poorer (R = 0.71) within the time window (ii). Using the time window (i)*[t − 3 h; t + 3 h]*, a statistically significant correlation (R = 0.82) is found between water vapour flux and rainfall obtained from radar measurements (when considering only radar data at ANETZ stations). This correlation becomes weaker when averaging radar data by using the time window (ii) *[t; t + 6 h]* (R = 0.66).

The fact that there is reasonably good correlation between $(-\partial W/\partial t + Wv_{in} - Wv_{out})$ and the radar data sets, and even better correlation between $(-\partial W/\partial t + Wv_{in} - Wv_{out})$ and the ANETZ raingauge information (observed data only) give us confidence that our method of determining the water vapour fluxes of Switzerland from the mass balance approach is robust and could be applied to other case studies. The 28% difference between computed water vapour flux and rain

estimated from ANETZ can be partly explained by the high frequency signals in ANETZ data, which are smoothed out over the 6-hour ECMWF analyses (Fig. 8). The relatively poorer agreement with the radar products (i.e., RADAR and CPC data) might indicate that i) the large spatial window used to compute the water vapour storage omits rain gauge or radar data outside Switzerland which may lead to some underestimations of the observed fluxes and ii) the radar precipitation algorithm for Switzerland still needs refining – although no doubt this would be extremely difficult in such a mountainous country. As mentioned earlier, the MeteoSwiss radar product has already undergone significant adjustment (e.g., GERMANN et al., 2006; FREI et al., 2006; SIDERIS et al., accepted).

To investigate the sensitivity of the rain-flux (as derived from the observations) to the size of the spatial window used for the computation of the water-vapour flux, we have selected 5 additional differently-sized spatial windows (pertinent to the spatial coverage of the precipitation) that permit us to examine the magnitude of the uncertainties between the computed water-vapour flux and rain-flux as derived from the observations. Figs. 8 (large spatial window), 9 (medium window), and 10 (a smaller window) illustrate the results of these analyses. Overall, the following conclusions are found:

(i) The water vapour fluxes derived from the ERA-Interim are larger than those derived from observed rainfall products including radar measurements, and that the ratio between the two increases as the window size gets smaller. The ratio is about 0.6 (Fig. 8) and 0.84 (Fig. 10) and can reach up to 0.9 (not shown), with relatively large ratios for CPC data. At the same time, however, we must realise that by decreasing the size of the spatial window, we are using much fewer gridpoints of ERA-interim data information which is coarse at 0.5 deg lat/lon. In addition the water-vapour flux is smoothed temporally with respect to the rain-flux, and this is visible especially during the first half of the time period when the rain events were short lived.

(ii) The observed mean rain-flux derived either from rain gauges or from the combined rain-gauge and radar when using only radar pixels at rain gauges locations decreases as the spatial window becomes smaller (or inside Switzerland). The ratio between rain gauge (combined rain-gauge and radar) data is found to be 1.28 (0.71) from Fig. 8 and it drops to about 0.47 (Fig. 10). The limited spatial sampling of the rain gauge network may explain these results in which a small scale precipitation structure can be missed.

Finally, because water vapour is an invisible gas and remains unseen, it is perhaps interesting to relate the amount of atmospheric water vapour transport across Switzerland to an everyday visible water entity, such as

Lake Geneva, for example. Lake Geneva itself has a volume of 89 km^3 and if this water was spread entirely evenly over the complete surface area of Switzerland (41,290 km^2, assuming a flat surface), the depth of water would be 2.155 metres, which is equivalent to 2,155 mm of integrated water vapour in atmospheric terms. As stated earlier, the mean value of the computed 6-hourly water vapour fluxes $(-\partial W/\partial t + Wv_{in} - Wv_{out})$ from ECMWF data is 0.32×10^8 kg/s; this is the mass of water passing through the Switzerland box per second, or about 2.8×10^{12} kg per day. As the mass of Lake Geneva is approximately 8.9×10^{13} kg in weight, so this means that the entire mass of Lake Geneva passes through Switzerland as water vapour about once every 32 days (or about once a month).

4   Conclusions and future outlook

The water vapour flux through Switzerland is highly temporally variable, ranging from 1 to 5×10^7 kg/s during quiet spells of weather, but increasing by a factor of 10 or more during high speed currents of water vapour, also known as "*warm air conveyer belts*" or "*atmospheric rivers*". The flux into Switzerland *(Wv$_{in}$)* is generally greater than the flux out (Wv_{out}). However, the difference is only a small fraction (1% to 5%) of the total water vapour flux. This indicates that Switzerland "imports" more water than it "exports", but the amount gained (*i.e.* probably through precipitation) remains only a small fraction of the total available water vapour passing by. An important finding is that high inward water vapour fluxes (Wv_{in}) are not necessarily linked to high precipitation episodes; a precipitation mechanism is also needed.

During the Swiss floods of August 2005, there is a noticeable shortfall (up to 30%) in modelled water vapour exiting Switzerland compared to that incoming, suggesting about one quarter to one third of the incoming water vapour got precipitated during the flood event – an efficiency that is comparable to Atlantic hurricanes (MEHTA et al., 2006). The water vapour mass balance $(-\partial W/\partial t + Wv_{in} - Wv_{out})$ during the August 2005 floods compare well with the the mean ANETZ rain gauge observations and with the MeteoSwiss combined rain-gauge and radar products.. In the case of very heavy rainfall and low air temperatures (such as during the August 2005 flood event), the approximation of the precipitation over Switzerland by only ($Wv_{in} - Wv_{out}$) is reasonable. Hence, the transient component$(-\partial W/\partial t)$, the evaporation (E), the liquid (Lw_{in} and Lw_{out}) and solid (Iw_{in} and Iw_{out}) water components in the Equation (3) can be considered to be small when estimating the precipitation. The water vapour mass balance $(-\partial W/\partial t + Wv_{in} - Wv_{out})$ approach used in this study can also indirectly help to discriminate between precipitation due to local convection and atmospheric currents of water vapour, as such happened during the August 2005 flood event.

Finally, high spatial resolution of meteorological data from e.g., ECMWF T799 model can help to refine the amplitudes of the computed water vapour fluxes, especially over a complex terrain like a Swiss country.

In future studies, it would be worthwhile to examine the very detailed daily TROWARA microwave record kept at the Institute of Applied Physics, University of Bern (MORLAND et al., 2009; MÄTZLER and MORLAND, 2009) to examine the temporal characteristics of peaks and troughs of the water vapour flux together with the integrated water vapour tendency. The TROWARA data has very high temporal resolution, which is more than four magnitudes greater than the ECMWF data used in this study (two seconds compared to six-hours). Daily hard copies of the TROWARA record, annotated with references to the daily weather for all times since January 2004 until today are available as a resource at the Institute of Applied Physics at the University of Bern. Also available are webcam sky images for Bern, taken every 7 minutes for the same period, revealing the cloud and weather conditions throughout this period (GRAHAM and KOFFI, 2009; GRAHAM et al., 2012).

The availability and use of wind profiler data would also be of an advantage in any future study. It would also be interesting to relate the peaks of Wv_{in} and Wv_{out} to Meteosat Second Generation water vapour imagery (*e.g.* 6.2 µm channel) and gauge any degree of correlation between them. Also Global Positioning System (GPS) integrated water vapour could be used as observations to independently confirm the $(-\partial W/\partial t + Wv_{in} - Wv_{out})$ balance (MORLAND and MÄTZLER, 2007; GRAHAM and KOFFI, 2009).

Acknowledgments

References

BENTON, G.S., M.A. ESTOQUE, 1954: Water-vapour transfer over the North American continent. – J. Meteor. **11**, 462–477.

BRUBAKER, K.L., D. ENTEKHABI, P. EAGLESON, 1993: Estimation of continental precipitation recycling. – J. Climate **6**, 1077–1089.

CADET, D., G. REVERDIN, 1981: Water vapour transport over the Indian Ocean during summer 1975. – Tellus **33**, 476–487.

CONNOLLEY, W.M., J.C. KING, 1993: Atmospheric water vapour transport to Antarctica inferred from radiosondes. – Quart. J. Roy. Meteor. Soc. **119**, 325–342.

CULLATHER, R.I., D.H. BROMWICH, M.L. van WOERT, 1996: Interannual variations in Antarctic precipitation related to El Nino–Southern Oscillation. – J. Geophys. Res. **101**, 19109–19118.

DAI, A.G., K.E. TRENBERTH, 2002: Estimates of freshwater discharge from continents: Latitudinal, seasonal variations. – J. Hydrometeor. **3**, 660–687.

DEE, D.P., S.M. UPPALA, A.J. SIMMONS, P. BERRISFORD, P. POLI, S. KOBAYASHI, U. ANDRAE, M.A. BALMASEDA, G. BALSAMO, P. BAUER, P. BECHTOLD, A.C.M. BELJAARS, L. van de BERG, J. BIDLOT, N. BORMANN, C. DELSOL, R. DRAGANI, M. FUENTES, A.J. GEER, L. HAIMBERGER, S.B. HEALY, H. HERSBACH, E.V. HÓLM, L. ISAKSEN, P. KÅLLBERG, M. KÖHLER, M. MATRICARDI, A.P. MCNALLY, B.M. MONGE-SANZ, J.-J. MORCRETTE, B.-K. PARK, C. PEUBEY, P. de ROSNAY, C. TAVOLATO, J.-N. THÉPAUT, F. VITART, 2011: The ERA-Interim reanalysis: configuration and performance of the data assimilation system, – Quart. J. Roy. Meteor. Soc. **137**, 553–597. doi: 10.1002/qj.828.

FREI, C., 2006; Eine Länderübergreifende Niederschlagsanalyse zum August Hochwasser 2005. Ergänzung zum Arbeitsbericht 211. – Arbeitsberichte der MeteoSchweiz 213, 10 pp., www.meteoschweiz.admin.ch/web/de/forschung/publikationen/alle_publikationen/eine_laenderuebergreifende.Par.0001.DownloadFile.tmp/ab213.pdf.

FREI, C., U. GERMANN, S. FUKUTOME, M. LINIGER, 2008: Möglichkeit und Grenzen der Niederschlagsanalyse zum Hochwasser 2005. – Arbeitsberichte der MeteoSchweiz 221, 21 pp., www.meteoschweiz.admin.ch/web/de/forschung/publikationen/alle_publikationen/ab-221.Par.0001.DownloadFile.tmp/ab221.pdf.

GERMANN, U., G. GALLI, M.Bolliger. BOSCACCI, 2006: Radar precipitation measurement in a mountainous region. – Quart. J. Roy. Meteor. Soc. **132**, 1669–1692.

GRAHAM, E., E. KOFFI, 2009: An observational study of air and water vapour convergence over the western Alps during summer and the development of isolated thunderstorms. – IAP Research Report No. 2009-01-MW, Institut für angewandte Physik, Universität Bern, online available at www.iap.unibe.ch/publications/publication.php?lang=en.

GRAHAM, E., E. KOFFI, C. MÄTZLER, 2010: The water vapour flux of Switzerland. – IAP Research Report No. 2010-03-MW, Institut für angewandte Physik, Universität Bern, 2010, online available at www.iap.unibe.ch/publications/publication.php?lang=en.

———, 2012: An observational study of air and water vapour convergence over the Bernese Alps, Switzerland, during summertime and the development of isolated thunderstorms. – Meteorol. Z. **21**, 561–574.

GUEROVA, G., E. BROCKMANN, F. SCHUBIGER, J. MORLAND, C. MÄTZLER, 2005: An Integrated Assessment of Measured and Modeled Integrated Water Vapor in Switzerland for the Period 2001–03. – J. Appl. Meteor. **44**, 1033–1044.

HASTENRATH, S., 1986: On climate prediction in the Tropics. – Bull. Amer. Meteor. Soc. **67**, 696–702.

JOSS, J., B. SCHÄDLER, G. GALLI, R. CAVALLI, M. BOSCACCI, E. HELD, G. BRUNA, G. KAPPENBERGER, V. NESPOR, R. SPIESS, 1997: Operational use of radar for precipitation measurements in Switzerland. – MeteoSwiss Report, online available at www.meteosuisse.admin.ch/web/fr/meteo/temps_actuel/image_radar/informations.Related.0001.DownloadFile.tmp/onlinedocumentation.pdf.

KHATEP, M.M., B.B. FITZHARRIS, W.E. BARDSLEY, 1984: Water vapour transfer over the southwest Pacific: Mean patterns and variations during wet and dry periods. – Mon. Wea. Rev. **112**, 1960–1975.

LONFAT, M., F.D. MARKS, S.S. CHEN, 2004: Precipitation distribution in tropical cyclones using the Tropical Rainfall Measuring Mission (TRMM) microwave imager: A global perspective. – Mon. Wea. Rev. **132**, 1645–1660.

MÄTZLER, C., J. MORLAND, 2009: Refined physical retrieval of integrated water vapour and cloud liquid for microwave radiometer data. – IEEE Trans. Geosci. Remote Sens. **47**, 1585–1594.

MATSUYAMA, H., T. OKI, M. SHINODA, K. MASUDA, 1994: The seasonal change of the water budget in the Congo River basin. – J. Meteor. Soc. Japan. **72**, 281–299.

MEHTA, A.V., E.A. SMITH, G. TRIPOLI, 2006: Precipitation efficiency of hurricanes over Gulf of Mexico and Caribbean Sea basins. – Geophys. Res. Abstracts **8**, 10309, www.cosis.net/abstracts/EGU06/10309/EGU06-J-10309.pdf.

MORLAND, J., C. MÄTZLER, 2007: Spatial interpolation of GPS integrated water vapour measurements made in the Swiss Alps. – Meteor. Appl. **14**, 15–26.

MORLAND, J., M. COLLAUD-COEN, K. HOCKE, P. JEANNET, C. MATZLER, 2009: Tropospheric water vapour above Switzerland over the last 12 years. – Atmos. Chem. Phys. **9**, 5975–5988.

NEIMAN, P.J., F.M. RALPH, A. GARY, G.A. WICK, D. JESSICA, J.D. LUNDQUIST, M.D. DETTINGER, 2008: Meteorological characteristics and overland precipitation impacts of atmospheric rivers affecting the west coast of North America based on eight years of SSM/I Satellite Observations. – J. Hydrometeor. **9**, 22–47.

PHILLIPS, I.D., G.R. MCGREGOR, 2001: Western European Water Vapor Flux–Southwest England Rainfall Associations. – J. Hydrometeor. **2**, 505–524.

SAHA, K.R., S.N. BAVADEKAR, 1973: Water vapour budget and precipitation over the Arabian Sea during summer. – Quart. J. Roy. Meteor. Soc. **99**, 273–278.

SCHMITZ, J.T., S.L. MULLEN, 1996: Water vapor transport associated with the summertime North American monsoon as depicted by ECMWF analyses. – J. Climate **9**, 1621–1634.

SENEVIRATNE, S.I., P. VITERBO, D. LÜTHI, C. SCHÄR, 2004: Inferring changes in terrestrial water storage using ERA-40 reanalysis data: The Mississippi River basin. – J. Climate **17**, 2039–2057.

SIDERIS, I.V., M. GABELLA, R. ERDIN, U. GERMANN, accepted: Real-time radar-raingauge merging using spatiotemporal co-kriging with external drift in the alpine terrain of Switzerland. – Quart. J. Roy. Meteor. Soc.

SIMMONDS, I., P. HOPE, 1998: Seasonal and regional responses to changes in Australian soil moisture conditions. – Int. J. Climatol. **18**, 1105–1139.

SIMMONDS, I., D. BI, P. HOPE, 1999: Atmospheric water vapour flux and its association with rainfall over China in summer. – J. Climate **12**, 1353–1367.

SMIRNOV, V.V., G.W.K. MOORE, 1999: Spatial and temporal structure of atmospheric water vapour in the Mackenzie River. – J. Climate **12**, 681–696.

STARR, V.P., J.P. PEIXOTO, 1958: On the global balance of the water vapour and hydrology of deserts. – Tellus **10**, 188–194.

TRENBERTH, K.E., C.J. GUILLEMOT, 1996: Physical processes involved in the 1988 drought and 1993 floods in North America. – J. Climate **9**, 1288–1298.

UPPALA, S.M., P.W. KALLBERG, A.J. SIMMONS, U. ANDRAE, V. DA COSTA, P. BECHTOLD, M. FIORINO, J.K. GIBSON, A. HERNANDEZ, G.A. KELLY, X. LI, K. ONOGI, S. SAARINEN, N. SOKKA, R.P. ALLAN, E. ANDERSSON, K. ARPE, M.A. BALMASEDA, A.C.M. BELJAARS, L. VAN DE BERG, J. BIDLOT, N. BORMANN, S. CAIRES, F. CHEVALLIER, A. DETHOF, M. DRAGOSAVAC, M. FISHER, M. FUENTES, S. HAGEMANN, E. HÓLM, B.J. HOSKINS, L. ISAKSEN, P.A.E.M. JANSSEN, R. JENNE, A.P. MCNALLY, J.-F. MAHFOUF, J.-J. MORCRETTE, N.A. RAYNER, R.W. SAUNDERS, P. SIMON, A. STERL, K.E. TRENBERTH, A. UNTCH, D. VASILJEVIC, P. VITERBO, J. WOOLLEN, 2005: The ERA-40 re-analysis. – Quart. J. Roy. Meteor. Soc. **131**, 2961–3012.

WANG, M., J. PAEGLE, 1996: Impact of analysis uncertainty upon regional atmospheric moisture flux. – J. Geophys. Res. **101**, 7291–7303.

ZANGVIL, A., P.J. LAMB, D.H. PORTIS, F. JIN, S. MALKA, 2010: Comparative study of atmospheric water vapor budget associated with precipitation in Central US and eastern Mediterranean. – Advanc. Geosci. **23**, 3–9.

ZHOU, T.-J., R.C. YU, 2005: Atmospheric water vapour transport associated with typical anomalous summer rainfall patterns in China. – J. Geophys. Res. **110**, D08104, doi:10.1029/2004JD005413.